

Article

Monitoring Spatial and Temporal Dynamics of Flood Regimes and Their Relation to Wetland Landscape Patterns in Dongting Lake from MODIS Time-Series Imagery

Yanxia Hu ^{1,2}, Jinliang Huang ^{1,*}, Yun Du ¹, Pengpeng Han ^{1,2} and Wei Huang ^{1,2}

¹ Institute of Geodesy and Geophysics, Chinese Academy of Sciences, Wuhan 430077, China; E-Mails: huyanxia2009@163.com (Y.H.); duyun@whigg.ac.cn (Y.D.); hanpeng2010@yeah.net (P.H.); vivian090414@sina.com (W.H.)

² University of Chinese Academy of Sciences, Beijing 100049, China

* Author to whom correspondence should be addressed; E-Mail: jin_liang_huang@163.com; Tel.: +86-27-6888-1360.

Academic Editors: George P. Petropoulos and Prasad S. Thenkabail

Received: 28 December 2014 / Accepted: 29 May 2015 / Published: 5 June 2015

Abstract: Dongting Lake, the second largest freshwater lake in China, is well known for its rapid seasonal fluctuations in inundation extents in the middle reach of the Yangtze River, and it is also the lake most affected by the Three Gorges Project. Significant inter-annual and seasonal variations in flood inundations were observed from Moderate Resolution Imaging Spectroradiometer (MODIS) time-series imagery between 2000 and 2012 in the Dongting Lake. Results demonstrated that temporal changes in inundation extents derived from MODIS data were accordant with variations in annual and monthly precipitation and runoff data. Spatial and temporal dynamics of some related parameters of flood regime were analyzed as well, which included flood inundation probability, duration and start/end date of the annual largest flood. Large areas with high flood inundation probability were identified in 2000 and 2002, but relatively small regions with great flood inundation probability occurred in 2001, 2006, and 2011. Long flood durations were observed in 2000, 2002, 2008, 2010, and 2012, whereas short flood durations occurred in 2001, 2006, and 2011. Correlation analysis techniques were applied to explore spatial-temporal relationships between parameters associated with flood regime and wetland landscape patterns from 2000 to 2012. In addition, this paper presented comprehensive discussions on development of related parameters of flood regime and their influences on wetland landscape pattern after impoundment of the Three Gorges Reservoir, changes in wetland

landscape patterns after the flood period, and the role of flooding in wetland evolution and vegetation succession. These results can provide scientific guidance and baseline data for wetland management and long-term monitoring of wetland ecological environment in the Dongting Lake.

Keywords: MODIS; flood inundation probability; duration; wetland landscape pattern

1. Introduction

The mechanism of vegetation succession is a part of the most important theoretical foundations for wetland restoration and conservation, and has become a central issue of wetland science [1–7]. Although several factors (such as soil nutrients and moisture, as well as the predation, competition, and promotion among wetland plants) influence the succession of wetland vegetation, hydrological conditions are the most significant and complicated elements [8,9]. Wetland hydrology is a major component of the wetland ecosystem, which primarily includes water-level fluctuation, flood inundation probability, hydro-period related variables (start time, duration, and end time of flood), and sedimentary material. In general, the wetland landscape pattern can present spatial distribution of wetland landscape patches for adapting to hydrological processes at different levels [10]. Moreover, the abovementioned water regimes are key factors for spatial differentiation of wetland landscape patterns, which exert pronounced influence on succession of wetland vegetation and benefits of wetland ecosystem [11–13], especially for lakes that experience obvious seasonal variations in inundation extents and those that are connected to large rivers.

Some studies supported by observation data have indicated that some changes have appeared in flood regimes in the Dongting Lake after impoundment of the Three Gorges Reservoir [14–18]. The annual runoff in the Yangtze River generally is distributed evenly by lowering water levels in the flood period and raising water levels in the dry period. Runoff and sediment flowing into the Dongting Lake from the Yangtze River have experienced a dramatic drop since the launch of the Three Gorges Project. With the changing water levels in the Yangtze River and the regulation of the Three Gorges Reservoir, wetlands in the Dongting Lake have been periodically or permanently affected by flooding. First, seasonal variations in floods determine varying degrees of flood inundation probability for wetland plants in diverse locations, which could have significant effects on the growth and spatial distribution of wetland vegetation. Second, flood duration and its start/end time could exert profound influence on biomass accumulation of wetland vegetation in different growth stages. The time interval between the end date of current flooding and the start date of subsequent flooding could also have considerable effects on wetland landscape patterns [19]. Third, given that the input and output of runoff are the main material exchanges for wetlands with the outside environment, sedimentary materials brought by floods could lead to depositions or erosions of wetlands and thus could accelerate developments or degradations of wetlands over a long period of time. Studies have shown that long-term floods would have tremendous effects on the processes of wetland evolution and vegetation succession [20–23]. In general, wetlands enduring erosion would tend to be replaced with submerged plants, whereas wetlands suffering sedimentation would have a trend of being substituted by emergent

plants. Specifically, reeds and poplars grown in middle–high wetlands would be transferred into meadows when experiencing long-term inundation, whereas meadow wetlands would be invaded by woody plants in the absence of periodic floods [24].

Therefore, dynamic monitoring flood regime has great theoretical and practical significance in understanding succession laws of wetland vegetation and ecological functions of wetlands [13,25,26]. Considerable research has utilized multi-temporal remote sensing imagery, especially Moderate Resolution Imaging Spectroradiometer (MODIS) data with high temporal resolutions, to monitor periodic fluctuations in hydrological conditions [27–33]. MODIS launched in December 1999 can view the surface of the entire Earth every one to two days, which is helpful in monitoring spatial and temporal dynamics of flood regimes at a regional scale [34–37]. MODIS imagery has two principal superiorities over other data sources. First, MODIS data can help understand inter-annual and seasonal changes in the hydrological environment of an entire lake from a global viewpoint, which cannot be achieved by traditional hydrographic surveys with a finite number of monitoring sites. Second, MODIS images with high temporal and spectral resolutions are more effective in identifying water pixels and monitoring frequent fluctuations in wetland environment than other remote sensing imagery with high spatial resolutions (Landsat, SPOT, Quickbird, *etc.*) [38,39].

The increase or decrease in water flows from the Three Gorges Reservoir changes the flood regime in the Dongting Lake, which would have beneficial or adverse effects on wetland vegetation. Numerous studies have investigated the changes in the wetland environment of the Dongting Lake in response to the Three Gorges Project, such as changes in water levels [40], hydrological environment [41], wetland vegetation biomass [42], and wetland ecosystem services [43]. A few studies have associated flood regimes with wetland landscape patterns as well. The current study, beyond previous applications of MODIS data, not only represented inter-annual and seasonal variations in inundation extents over the period during 2000 to 2012 in the Dongting Lake, but also derived other hydrological related factors (flood inundation probability, flood duration, and the start/end date of the annual largest flood) that are crucial to wetland landscape pattern. Quantitative analysis methods were applied to explore relationships between hydrological factors and wetland landscape patterns.

Our goal is to explore an efficient method to monitor changes in wetland vegetation patterns and thus to reflect modifications of the wetland environment resulting from the Three Gorges Project. Combination of long-term Terra/MODIS data with wetland landscape pattern data provided a feasible way to understand the spatial and temporal distributions of flood regimes of the Dongting Lake and to address the insufficiency of measurements from limited hydrologic stations. There were three major objectives in this study. The first was to develop an efficient approach for analyzing spatial and temporal characteristics of flood regimes in the Dongting Lake. The second was to establish relationships between flood regimes and wetland landscape patterns in the Dongting Lake. The third was to explore possible effects of the developments of flood regimes on wetland evolution and vegetation succession after running the Three Gorges Project.

Results of this study could establish baseline information for future estimation of flood regimes and provide data for other research. The applications of monitoring dynamics of flood regime and its relation to wetland landscape pattern are of great ecological and economic importance for management of the Three Gorges Reservoir and the enhancement of ecosystem services of wetlands in the Dongting Lake.

2. Study Area

The Dongting Lake ($28^{\circ}42'–29^{\circ}38'N$ and $111^{\circ}52'–113^{\circ}08'E$, Figure 1) is located in the north of Hunan Province and the south of middle reaches of the Yangtze River (Jing River). The lake has an area of 2794.7 km^2 and is the second largest freshwater lake in China. Runoff discharged into the Dongting Lake principally contains four tributaries (Xiang River, Zi River, Yuan River and Li River) and those diverted from the Yangtze River through three outlets (Songzi, Taiping and Ouchi), and discharged back into the Yangtze River at the northeast outlet (Chenglingji). These water supplies are mostly concentrated in the flood season from June to September [44]. The Dongting Lake experiences great seasonal variations in water levels because it is affected by the monsoon climate. The annual mean lowest water level is only 20.19 m, which often happens in January. By contrast, the annual mean highest water level can reach 30.24 m, which usually occurs in July [45]. The Dongting Lake is likely to be affected by the Three Gorges Project given its specific geographical location and hydrological connectivity.

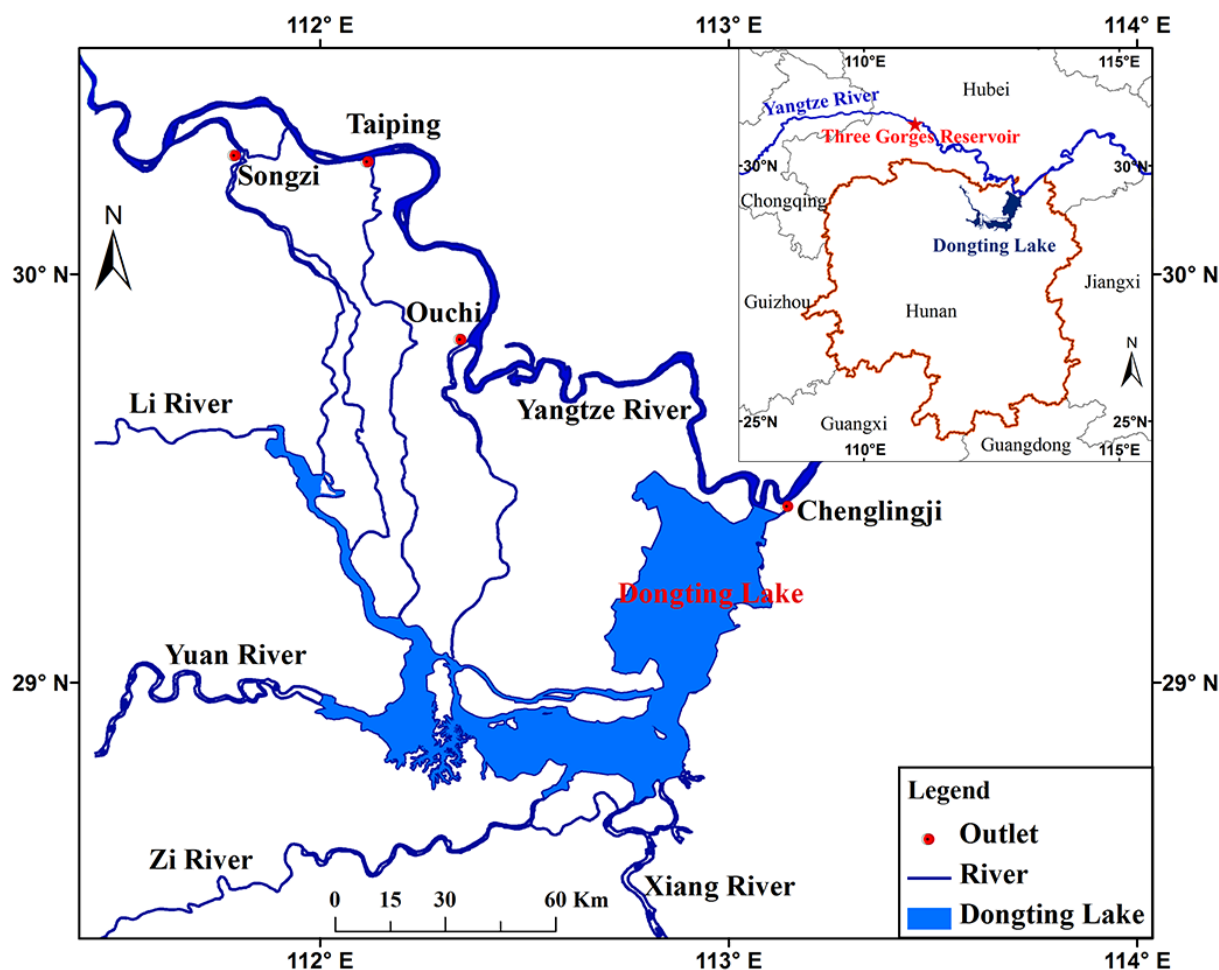


Figure 1. Geographical location and hydrological connectivity of the Dongting Lake. The red five-pointed star in the inset map indicates that the Dongting Lake is downstream of the Three Gorges Reservoir.

To adapt to the changing water levels, wetland plants are growing along water-level gradients with a zonal distribution [13,46–51]. The primary wetland vegetation communities from water to land are

submerged plants, phalaris (*Phalaris arundinacea*), carex (*Carex brevicuspis*), reed (*Phragmites australis*), and poplars (*Populus euramericana*) [52,53]. Only a few polygonum (*Polygonum flaccidum*) and artemisia (*Artemisia selengensis*) sporadically grow in some specific areas. In recent years, there was an expansion trend for poplars (*Populus euramericana*) planted in high wetlands, which would be a serious threat to the wetland ecological environment in the Dongting Lake.

3. Data and Materials

3.1. Remote Sensing Imagery

Terra/MODIS data used in this study involved MOD09GQ and MOD09GA daily reflectance products with resolutions of 250 and 500 m, respectively. These data were derived from the Land Processes Distributed Active Archive Center (LP DAAC) [54] of the United States National Aeronautics and Space Administration (US NASA). MOD09GQ contained two bands (648 and 858 nm), and MOD09GA included seven bands (648, 858, 470, 555, 1240, 1640, and 2130 nm). They were geo-referenced into a consistent projection of Universal Transverse Mercator (UTM) Grid System by MODIS Reprojection Tool (MRT) [55]. Given different resolutions for these two data sets, a “sharpening” scheme [56] was applied to resample the third to seventh bands of MOD09GA to a resolution of 250 m. These bands were then stacked with one to two bands of MOD09GQ to acquire 250 m data with seven bands, which would have an improved appearance of red-green-blue (RGB) images. We used a variety of cloud-removing methods but failed to obtain satisfactory results. Therefore, RGB composite images were used as the last resort to select cloudless images. A total of 4628 images were generated between 2000 and 2012, among which 445 cloud-free images were selected (Table 1). Most months consisted of an average of two to six available images, and only a few months had no image. Considerable cloudless images can be found in November because of the good weather.

Table 1. Number of cloudless MODIS images in each month from 2000 to 2012.

Month	2000	2001	2002	2003	2004	2005	2006	2007	2008	2009	2010	2011	2012
January	-	1	1	5	1	1	4	3	2	3	1	1	1
February	1	2	4	3	2	0	0	1	2	1	1	2	0
March	2	2	2	3	4	3	1	2	3	2	2	1	3
April	2	1	1	5	5	7	2	6	1	2	2	2	3
May	6	3	2	3	3	0	3	4	1	3	3	4	1
June	2	1	1	2	1	2	3	0	1	4	0	0	0
July	4	3	5	8	4	5	1	3	1	3	1	6	3
August	1	1	4	4	3	2	3	1	0	3	6	3	1
September	5	10	3	4	5	6	6	4	1	2	3	0	4
October	1	1	6	4	5	4	2	1	4	4	4	3	4
November	7	9	5	6	2	2	5	6	3	6	5	3	4
December	1	2	0	0	5	6	7	1	5	0	7	4	4
Cloudless	32	36	34	47	40	38	37	32	24	33	35	29	28
Total	293	346	355	356	364	364	364	365	361	364	365	365	366

Landsat Thematic Mapper (TM)/Enhanced TM Plus images (ETM+) with a resolution of 30 m were obtained from the United States Geological Survey (USGS) [57] covering the East Dongting Lake in 1993, 1996, 2002, and 2010, which were selected in the flood, normal, and dry seasons (Table 2). These images were geometrically rectified and reprojected into the same UTM coordinate as the above MODIS images. These data would be used to give an example of the role of flooding in accelerating the process of wetland evolution and vegetation succession in the Dongting Lake.

Table 2. Periods, paths, rows, acquisition dates, and sources of Landsat images.

Period	Path/Row	Date	Landsat
The flood season	123/40	08/17/1996	TM
		07/09/2002	ETM+
		08/03/2010	TM
The normal season	123/40	10/04/1996	TM
		10/13/2002	ETM+
		10/30/2010	TM
The dry season	123/40	12/31/1993	TM
		12/29/2001	ETM+
		01/02/2010	TM

3.2. Hydrological and Meteorological Monitoring Data

Average annual and monthly precipitation data during 2000 to 2012 over the study area were derived from the China Meteorological Data Sharing Service System [58], which primarily included four meteorological stations (Nanxian, Yueyang, Changde, and Yuanjiang). Average annual and monthly runoff data between 2000 and 2012 were obtained from the Sediment Bulletin of the Yangtze River [59], which involved Chenglingji hydrological station at the outlet of the Dongting Lake.

3.3. Auxiliary Data

Field sampling and wetland landscape pattern data were collected as auxiliary data in this study to explore relationships between related parameters of flood regime and wetland landscape pattern.

Field sampling data were accumulated in four periods (September 2010, October 2010, April 2013 and November 2013). These data were located by a handheld global positioning system (GPS) and matched to remote sensing images, which were geometrically rectified by experienced personnel who were familiar with the local field conditions. Polygon features derived from these measurements provided a qualitative assessment of the wetland vegetation conditions (such as wetland plant communities, biomass, and biodiversity). These field data would be used as the reference for combining classes into specified categories in the process of wetland classification.

Wetland landscape pattern data were derived from the research of Hu *et al.* (2014) [60]; they developed a rule-based model to extract the spatial distribution of wetland vegetation from MODIS time-series data during 2000 to 2012 in the Dongting Lake. Hu *et al.* (2014) [60] verified the accuracy of the wetland landscape pattern data and obtained an overall accuracy of 83.99% and a Kappa coefficient of 0.79.

4. Methods

4.1. Water Area Delineation

Spectral index is a common method for extracting water surface from remote sensing images [61–63]. The most widely used indices include normalized difference vegetation index (NDVI) [64], normalized difference water index (NDWI) [65] and modified NDWI (MNDWI) [66]. These indices, constructed by a ratio form (NDVI, NDWI, *etc.*), are sensitive to aerosols and solar elevation angles. Therefore, thresholds for distinguishing water from wetlands are often extremely varied between different images, and sometimes quite differ in the same image with dissimilar distributions of aerosols and solar elevation angles [35,67,68]. When confronted with a large number of images, extensive work cannot be achieved through batch processing. A steady-state index would be very useful for resolving these problems.

Hu (2009) [67] proposed such an index named floating algae index (FAI) and used this index to extract long time-series water boundaries in the Tai Lake. FAI can be calculated as follows:

$$FAI = R_{rc,nir} - R'_{rc,nir}; \quad (1)$$

$$R'_{rc,nir} = R_{rc,red} + (R_{rc,swir} - R_{rc,red}) \times (\lambda_{nir} - \lambda_{red}) / (\lambda_{swir} - \lambda_{red}). \quad (2)$$

where $R'_{rc,nir}$ is the baseline reflectance in the near-infrared band derived from a linear interpolation between red band and short-wavelength infrared band. This baseline reflectance is equivalent to making an atmospheric correction from the two bands. This study used the surface reflectance from MOD09GA/MOD09GQ instead of the Rayleigh-corrected reflectance to derive FAI. Since FAI was initially used to detect floating algae in global oceans, the effect of aerosols could be lowered by selecting cloudless images with good quality when it came to a more local inland lake. FAI can extract the water delineation with relatively uniform thresholds at spatial and temporal ranges and thus is efficient for batch-oriented processing of considerable data. Feng *et al.* (2012) [35] used this index combining with a gradient approach to extract the water body from MODIS data during 2000 to 2010 in the Poyang Lake with the thought of regarding the maximum gradient of FAI as the water/marshland boundary. On the basis of Feng's research, Hu *et al.* (2014) [60] utilized FAI with a gradient approach of Robert [69] to derive inundation areas from MODIS images between 2000 and 2012 in the Dongting Lake and Poyang Lake. In the current study, the method used for water area delineation was guided by that of Hu *et al.* (2014) [60]. Figure 2 presents a schematic view of this method for water extraction.

4.2. Flood Inundation Probability

Flood inundation probability was defined as the probability of a wetland pixel being inundated by flood waters during one year. The formula was as follows:

$$f = \left(\frac{1}{n}\right) \sum_{i=1}^n x_i \sim [0, 1] \quad (3)$$

where f denotes the flood inundation probability, n is the number of images in a year, x_i is the pixel value of i -th water image (0 for non-water and 1 for water) for a certain wetland pixel. This parameter

can reflect the relative bottom topography of wetlands. Wetlands having large values of flood inundation probability are usually associated with low elevations, and vice versa.

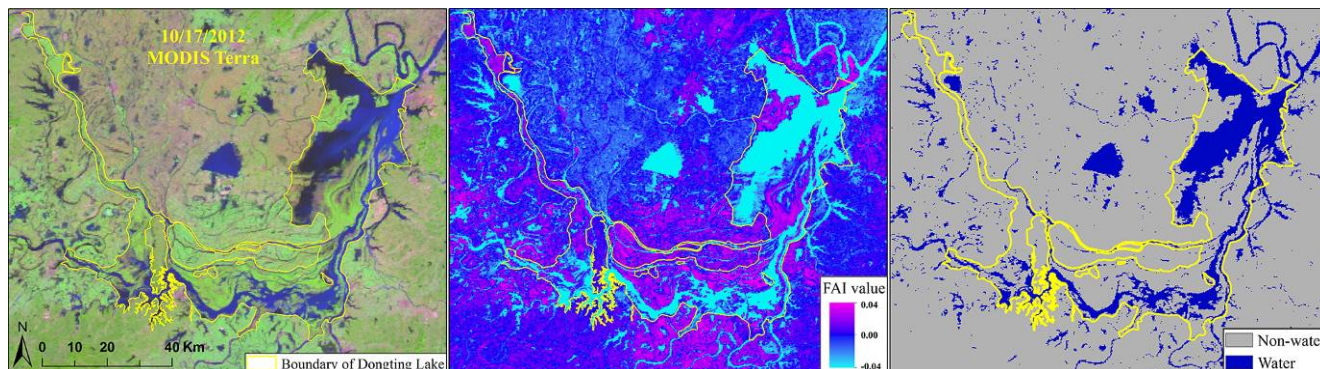


Figure 2. Process and result of water area delineation. The following figures from left to right were MODIS image on 17 October 2012, FAI image, and water image extracted by FAI gradient method.

4.3. Duration and Start/End Date of the Annual Largest Flood

The largest flood plays an important role in the spatial differentiation of wetland landscape patterns. To some extent, this phenomenon decides the outcropping vegetation type after being submerged. This study utilized daily MODIS imagery to detect the duration and start/end date of the annual greatest flood. Duration of the largest flood was defined as the longest period of continuous inundations, which was established as the time interval between the start date and end date of the annual largest flood:

$$d = \max(j - i + 1, x_j = \dots = x_{i+1} = x_i = 1) \quad (4)$$

where d denotes the flood duration, i is the start date for a certain wetland pixel, and j is the end date for a certain wetland pixel. For each wetland pixel, the continuous flood periods were first recorded by water-related pixels. Second, if periods of continuous inundation were identified twice or more in a year, the longer period would be taken as the annual largest flood. Third, the duration was defined from the start and end times of the annual largest flood. These three hydro-period related variables can be achieved by programming with MATLAB.

4.4. Wetland Landscape Patterns before and after the Flood Period

Changes in wetland landscape patterns can provide a comparative review of the adaptation and response of wetland plants to flooding stress, which can be observed in different phases of remote sensing images. This study made wetland classifications for several groups of MODIS images before and after the flood period to clarify the effect of floods on wetland landscape pattern in the Dongting Lake. Iterative self-organizing data analysis technique algorithm (ISODATA) was used to perform unsupervised classifications of MODIS images. We initially selected 10 classes, which would be combined into three general categories (reed, meadow, and tidal wetlands) with the help of field sampling data and expert knowledge. Reed wetlands were primarily composed of majorities of reeds and minorities of poplars, meadow wetlands mainly were consisted of carex and phalaris, and tidal

wetlands principally comprised mudflat and water. MODIS images for classification should be selected in April (before the flood period) and October (after the flood period) with equivalent inundation areas when floods were not large and most wetland plants were in the growing season.

5. Results

5.1. Inter-Annual and Seasonal Variations in Inundation Extents

Studies on spatial and temporal changes in inundation extents can enable a thorough understanding of the characteristic of expansion and recession of flood cycles at a regional scale. Only cloud-free images were selected to illustrate inter-annual and seasonal variations in inundation areas in consideration of the uneven distributions of clouds and noises. Figure 3 illustrates temporal changes in inundation areas gained from MODIS images with the lapse of day of year (DOY) between February 2000 and December 2012 in the Dongting Lake. There were significant variations in inundation extents over the period from 2000 to 2012 in Dongting Lake. Large scale floods with long durations could be observed in 2000, 2002, and 2003, with average inundation areas of 1342.0 km², 1329.0 km², and 1252.3 km², respectively. The wetlands almost experienced four massive floods in each year in these years. However, relatively small scale floods occurred in 2009, 2007, 2006, and 2011, with average inundation areas of 950.7 km², 810.8 km², 781.7 km², and 742.4 km², respectively. Annual inundation areas during these years were lower than the historical average level (1051.4 km²).

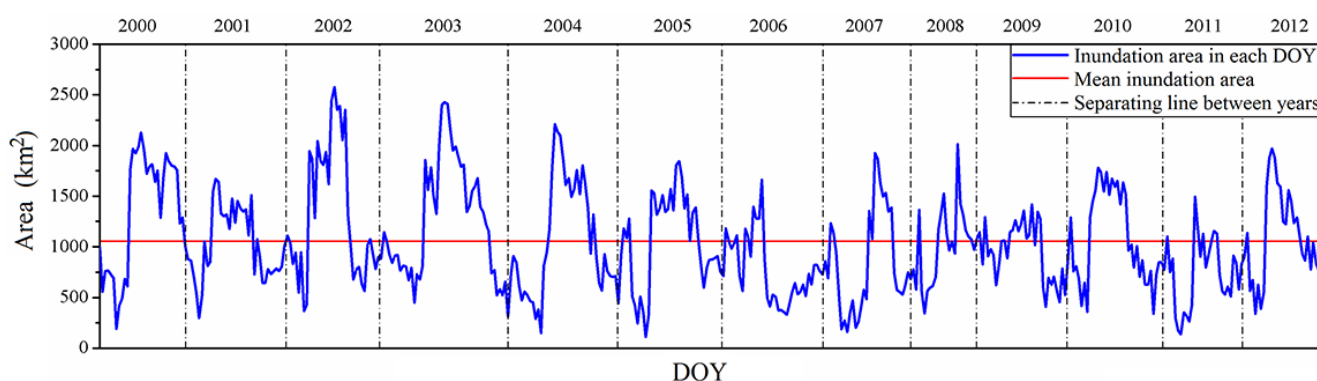


Figure 3. Temporal variations in inundation areas obtained from MODIS images between February 2000 and December 2012 in the Dongting Lake. The red line indicates the mean inundation area over the period from 2000 to 2012, and the dash dotted lines denote separating lines between years.

Temporal changes in inundation extents acquired from MODIS data are accordant with annual runoff and precipitation data recorded at the Chenglingji Station (Figure 4). Annual precipitation, runoff and inundation area all experience a downward trend, with a reduction rate of 41.1 mm·year⁻¹, 9.4 (10⁸m³)·year⁻¹, and 27.7 km²·year⁻¹, respectively.

Figure 5 presents the maximum (red plus blue) and minimum (red) inundation areas acquired from MODIS images in each month over the 13-year period, from 2000 to 2012. Both maximum and minimum inundation extents vary greatly from January to December. The flood period in the Dongting Lake is principally from June to September, with an average inundation area of 1508.8 km².

Both maximum and minimum inundation extents are large in June and July. The normal period is primarily in April, May, October, and November, with an average inundation area of 933.7 km². The dry period is mainly in January, February, March, and December, with an average inundation area of 747.3 km².

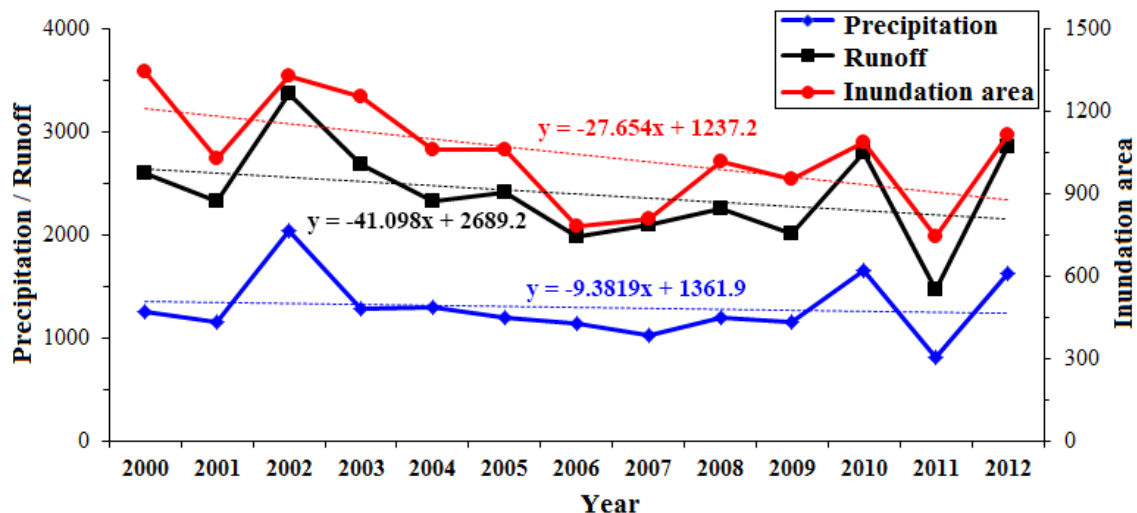


Figure 4. Temporal changes in annual precipitation, runoff and inundation areas acquired from MODIS data during 2000 to 2012 in the Dongting Lake. The dotted lines denote their development trends. (Precipitation: mm; Runoff: 10⁸ m³; Inundation area: km²).

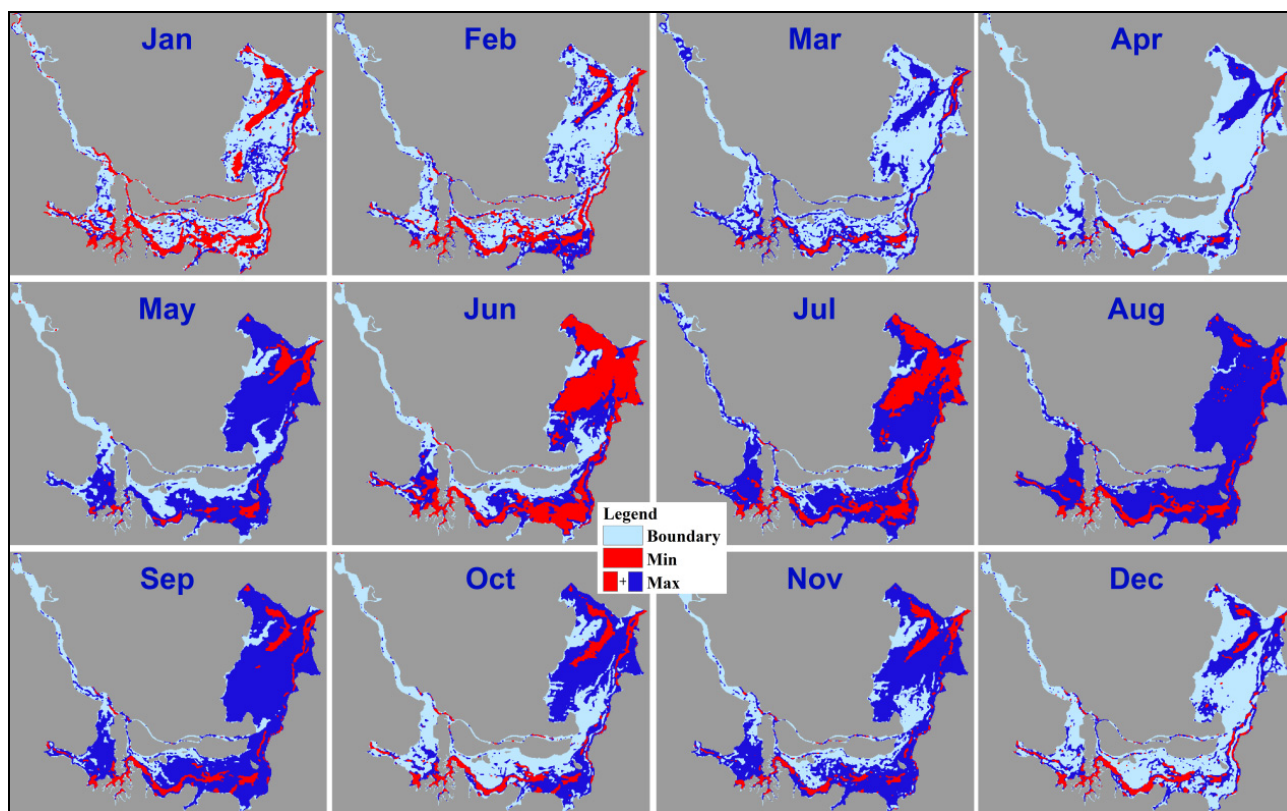


Figure 5. Variations in minimum and maximum inundation areas derived from MODIS images in each month during 2000 to 2012 in the Dongting Lake.

Considering that the water supply in the Dongting Lake is primarily gained from precipitation and runoff, we compared the average monthly precipitation, runoff, and inundation area obtained from MODIS data in each month between 2000 and 2012 in Figure 6. Similar tendencies exist among these three observations.

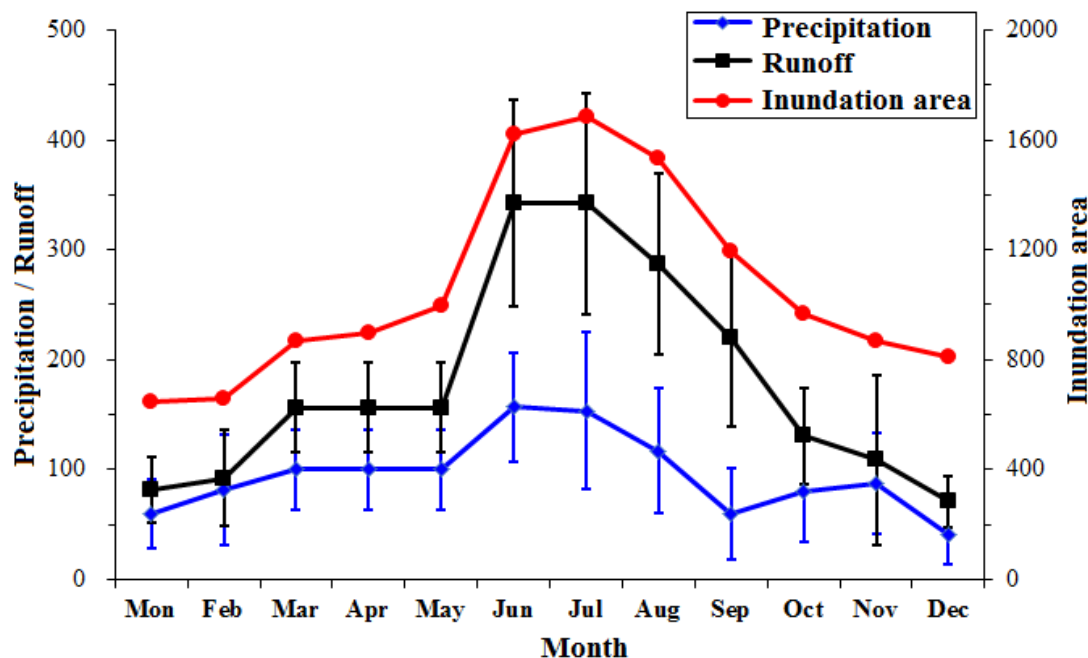


Figure 6. Changes in the average monthly precipitation, runoff, and inundation areas obtained from MODIS data between 2000 and 2012 in the Dongting Lake. The error bars represent standard deviations of precipitation and runoff. (Precipitation: mm; Runoff: 10^8 m^3 ; Inundation area: km^2).

5.2. Flood Inundation Probability and Its Relation to Wetland Landscape Patterns

The spatial distribution of flood inundation probability is helpful in identifying varying degrees of the effect of flooding on wetlands. Figure 7 shows the spatial and temporal variations in flood inundation probability of wetlands during 2000 to 2012 in the Dongting Lake. Large areas with high flood inundation probability are identified in 2000 and 2002, but relatively small areas with great flood inundation probability occurred in 2001, 2006, and 2011. The flood inundation probability also exhibits an obvious gradient distribution, which gradually decreases along the radial orientation from the lake center to the lake shore (Figure 7).

Spatial overlay analyses were used to investigate the relationship between flood inundation probability and wetland landscape patterns, which can be conducted by overlaying these two groups of data layers. Figure 8 manifests the variations in average areas of reed, meadow, and tidal wetlands with the change in flood inundation probability over the period 2000 to 2012 in the Dongting Lake. Significant differences can be observed among the three wetland types with the change in flood inundation probability. Variations in reed and tidal wetlands exhibit opposite trends. Approximately 92.4% of reed wetlands have a tolerance range of flood inundation probability between 0 and 0.3, whereas approximately 88.6% of tidal wetlands present a tolerance range of flood inundation

probability between 0.6 and 1. The flood inundation probability for meadow wetland is primarily between 0.3 and 0.6, and approximately 84.5% of meadow wetlands are distributed in this range.

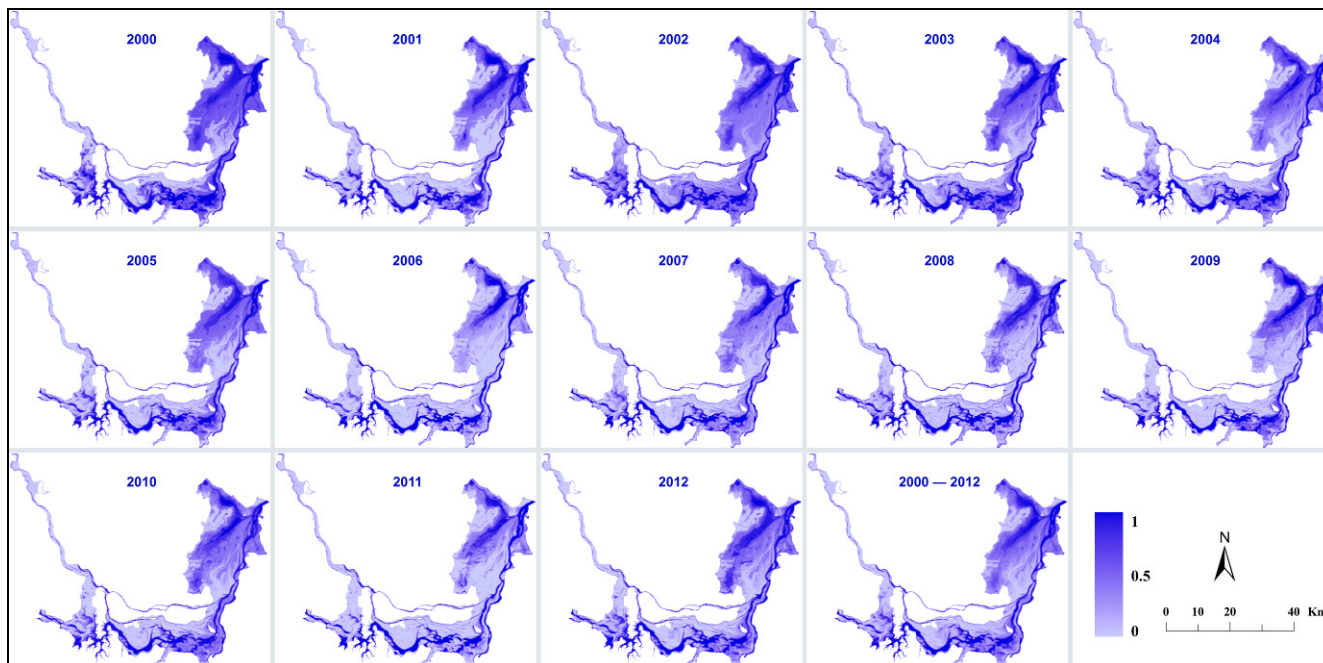


Figure 7. Spatial and temporal variations in flood inundation probability during 2000 to 2012 in the Dongting Lake.

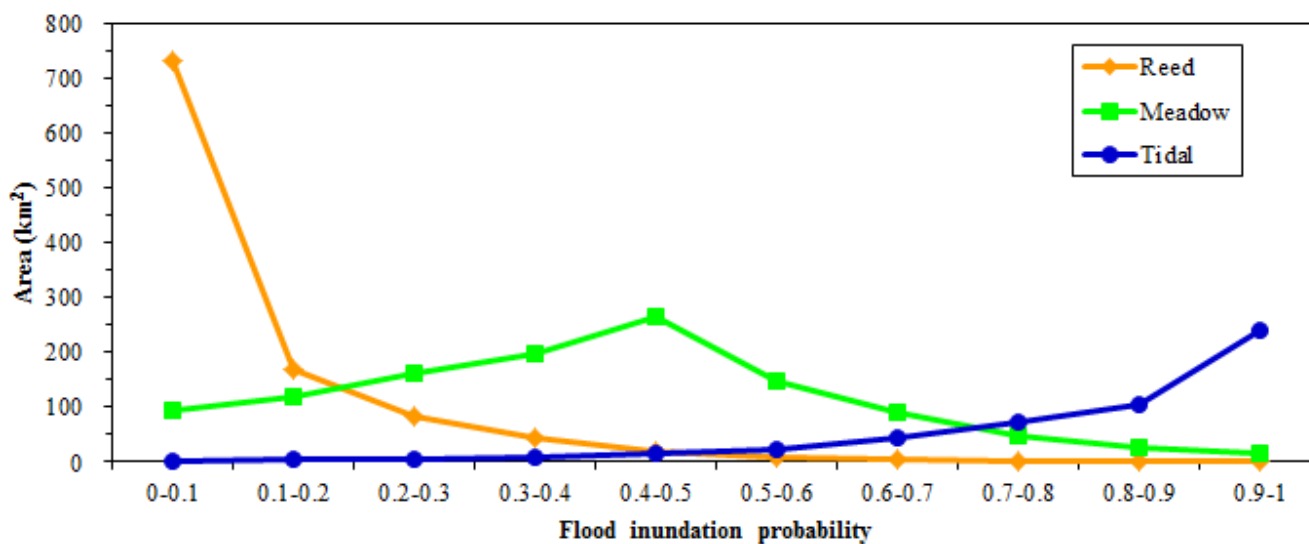


Figure 8. Variations in average areas of reed, meadow, and tidal wetlands with the change in flood inundation probability over the period from 2000 to 2012 in the Dongting Lake.

5.3. Spatial-Temporal Characteristics of the Annual Largest Flood

The spatial and temporal distributions of the duration and start/end date of the annual largest flood can provide a good way to identify characteristics of the greatest inundation cycles and regions most affected by floods. Figure 9 indicates the changes in the duration and start/end date of the largest flood from 2000 to 2012 in the Dongting Lake.

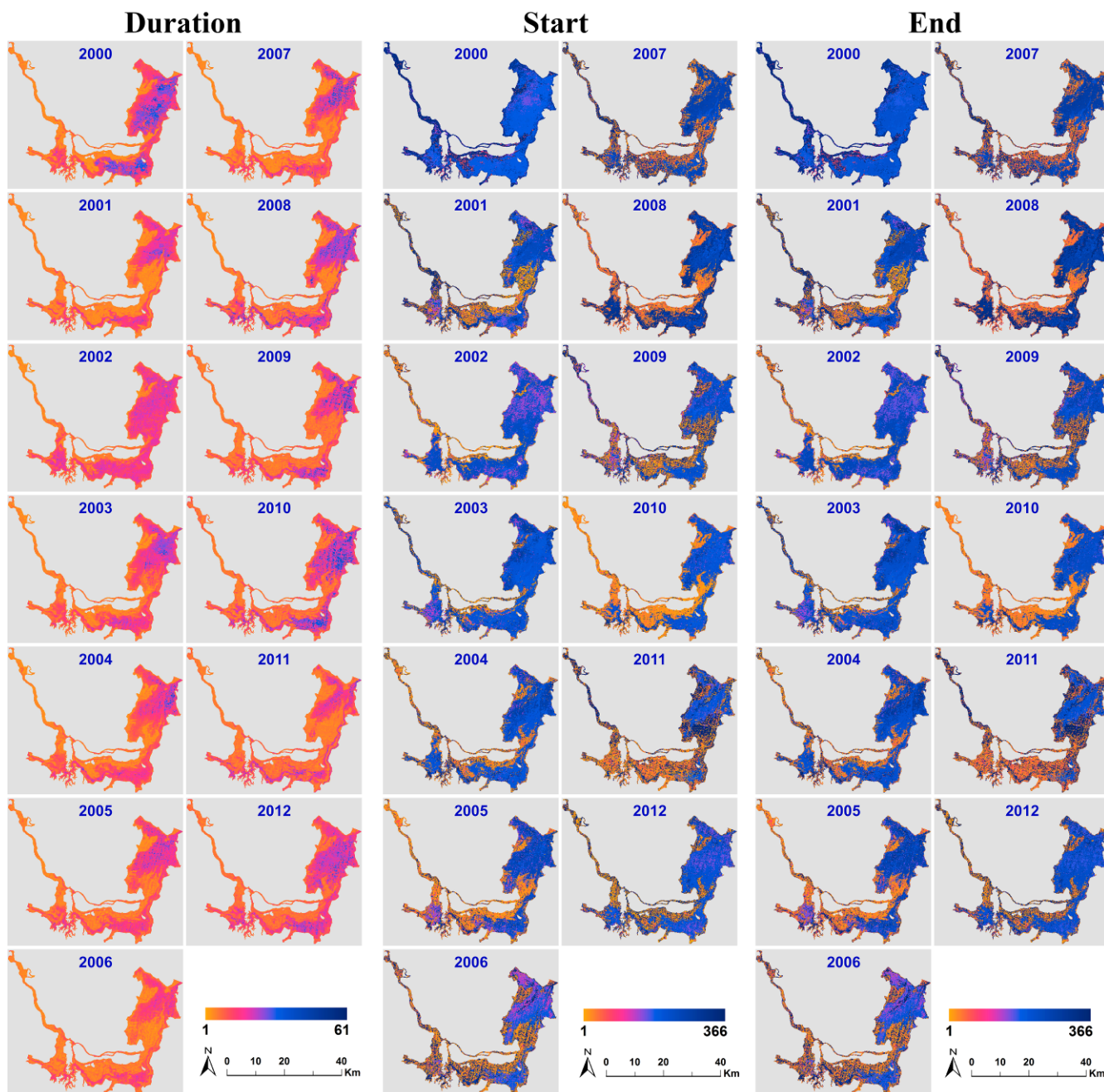


Figure 9. Spatial and temporal changes in the duration and start/end date of the largest inundation cycle from 2000 to 2012 in the Dongting Lake.

The flood duration (duration of the annual largest flood) varied among different years. Long durations were observed in 2000, 2002, 2008, 2010, and 2012, whereas short durations occurred in 2001, 2006 and 2011. These years with long or short durations of the annual largest flood appeared to be accordant with the years when the flood reached their peak points in an upward trend of inundation areas or decreased to their lowest levels in a downward trend of inundation extents. Wetlands with high flood inundation probability commonly experience long flood durations and vice versa. The start/end dates differ yearly but were consistent with each other. The start/end date of the largest flood occurred early in 2005, 2006, and 2010 but late in 2000, 2003, 2007, and 2008.

Spatial overlay analyses were applied to clarify relationships between the three parameters (duration, start date, and end date of the largest flood) and wetland landscape patterns, which can be implemented by overlaying three groups of data layers. Figure 10 displays the variations in average areas of reed, meadow, and tidal wetlands with the change in the duration and start/end date of the greatest flood from 2000 to 2012 in the Dongting Lake. The results were summarized below.

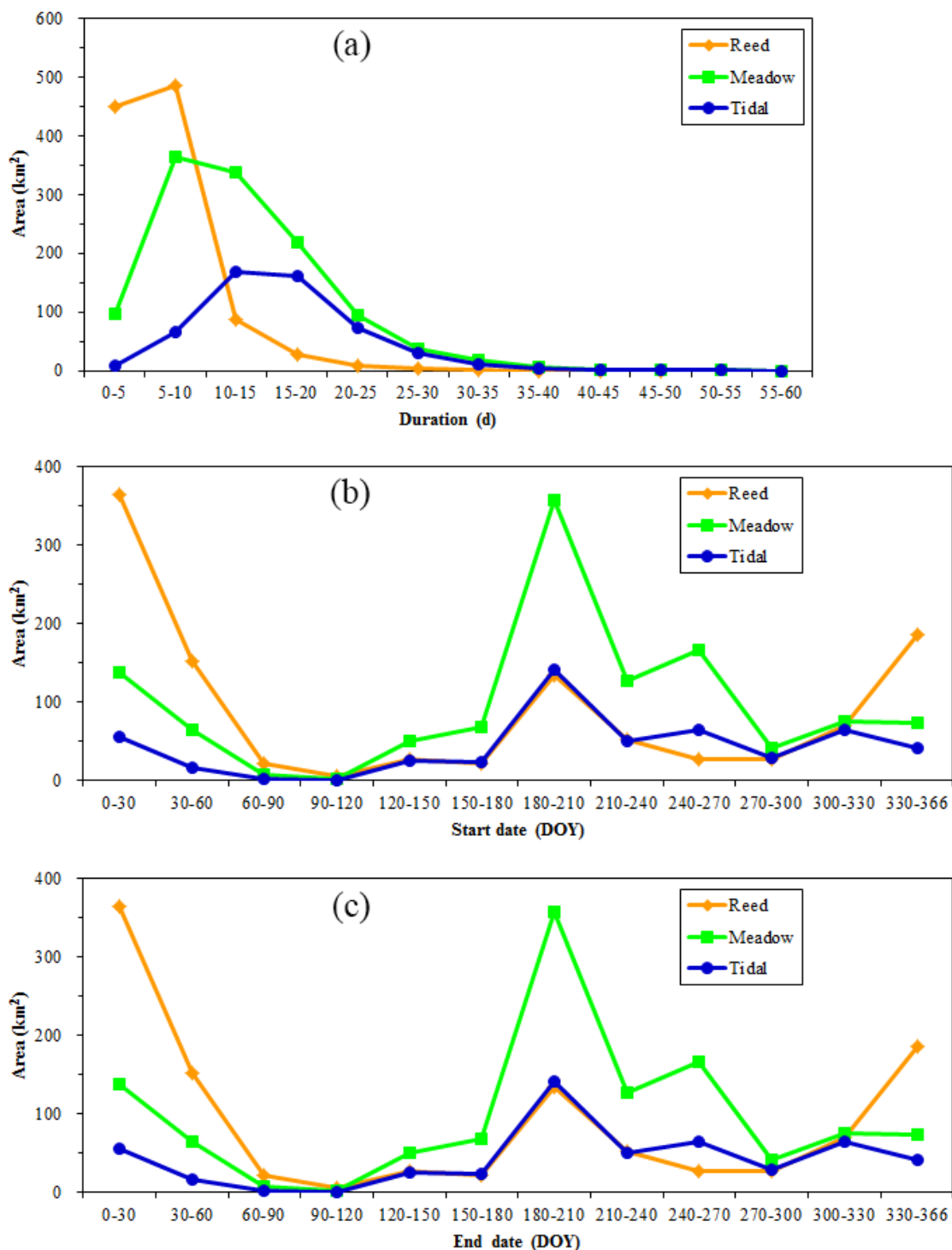


Figure 10. Variations in average areas of reed, meadow, and tidal wetlands with the change in the duration (a); start date (b); and end date (c) of the largest flood over the period from 2000 to 2012 in the Dongting Lake.

First, significant differences existed among various wetland types with the change in flood duration. Reed wetlands had poor water-resistance, and 87.8% of them showed a tolerance range of flood duration between one and 10 days. Meadow wetlands held better water-resistance than reed wetlands, and 78.2% of them presented a tolerance range of flood duration from five to 20 days. Tidal wetlands indicated greater water-resistance than reed and meadow wetlands, and 82.6% of them exhibited a tolerance range of flood duration between 10 and 30 days. When flood lasted over 45 days, the majority of reed and meadow wetlands would be submerged in floods, and tidal wetlands would be in the dominant position in the Dongting Lake.

Second, great variations can be observed among the three wetland types with the change in the start date of the largest flood. For reed wetlands, 47.2%, 19.6%, and 23.4% of them began to experience the largest flood in DOYs of 0 to 60 (January and February), 180 to 270 (July to September), and 300 to 366 (November and October), respectively. For meadow wetlands, 17.3%, 55.5%, and 12.7% of them went through the greatest flood in DOYs of 0 to 60, 180 to 270 and 300 to 366, respectively. For tidal wetlands, 13.9%, 49.7%, and 20.3% of them experienced the largest flood in DOYs of 0 to 60, 180 to 270 and 300 to 366, respectively. A large amount of wetland vegetation suffered the greatest inundation during July to September (DOYs 180 to 270), especially in July (DOYs 180 to 210). This period was the universal flood period and the main growing season of wetland vegetation in the Dongting Lake, which would exert significant influence on wetland landscape patterns. Specifically, 12.2% of reed wetlands, 30.4% of meadow wetlands and 27.3% of tidal wetlands experienced the largest flood in July.

Third, profound changes can be determined among wetlands with the change in the end date of the greatest flood. For floods that lasted two to three days at least, and one to two months at most, some differences existed in the influence of the start/end date of the largest flood on wetland landscape pattern. Statistics for the end date of the greatest flood were based on the same time ranges as the start date of the largest inundation. For reed wetlands, 46.3%, 19.4%, and 23.6% had the greatest flooding ending in in DOYs of 0 to 60, 180 to 270, and 300 to 366, respectively. For meadow wetlands, 18.4%, 51.9%, and 13.5% of them concluded their largest flood in DOYs of 0 to 60, 180 to 270, and 300 to 366, respectively. For tidal wetlands, 14.7%, 46.7%, and 24.7% of them completed the greatest flood in DOYs of 0 to 60, 180 to 270, and 300 to 366, respectively. A great deal of wetland vegetation ended the largest inundation during July to October (DOYs 180 to 300), especially in August (DOYs 210 to 240), in which 7.0% of reed wetlands, 23.9% of meadow wetlands, and 18.4% of tidal wetlands ended the greatest flood. Proportionate areas of the three wetland types ending the largest flood from July to September were less than those starting the greatest flood at the same time. By contrast, the proportions of areas of wetlands ending the largest flood in November and December were more than those starting the greatest flood at the same time. Such a difference was probably the result of time lag caused by the continued flooding.

5.4. Spatial-Temporal Correlations between Flood Regimes and Wetland Landscape Patterns

Correlation analyses were conducted to explore relationships between parameters associated with flood regime and wetland landscape patterns from 2000 to 2012. Such approach would provide an effective way to illustrate the impact of flooding on wetland vegetation and to identify the areas that

are most affected by floods. The formula for calculating the correlation coefficient between flood inundation probability and wetland landscape pattern is as follows:

$$r = \frac{\sum (F_i - \bar{F})(W_i - \bar{W})}{\sqrt{\sum (F_i - \bar{F})^2 \sum (W_i - \bar{W})^2}} \quad (5)$$

where F_i indicates the flood inundation probability in i -th year, W_i denotes a certain wetland landscape in i -th year, \bar{F} and \bar{W} present the average values of flood inundation probability and wetland landscape over the period from 2000 to 2012, respectively. The correlation coefficient between flood duration and wetland landscape pattern can be obtained through this formula as well. All these input parameters should be normalized before the calculation. Generally, $|r| \geq 0.8$ was considered to indicate a highly significant correlation, $0.5 \leq |r| < 0.8$ was considered to suggest a moderate correlation, $0.3 \leq |r| < 0.5$ was deemed to exhibit a low correlation and $|r| < 0.3$ was considered to present a weak or irrelevant correlation. $p < 0.05$ indicated a statistically significant result. In other words, large absolute values of correlation coefficients commonly demonstrated that variations in flood inundation probability and flood durations were highly correlated with spatial differentiations of wetland landscape patterns, and vice versa. The results are shown in Figure 11.

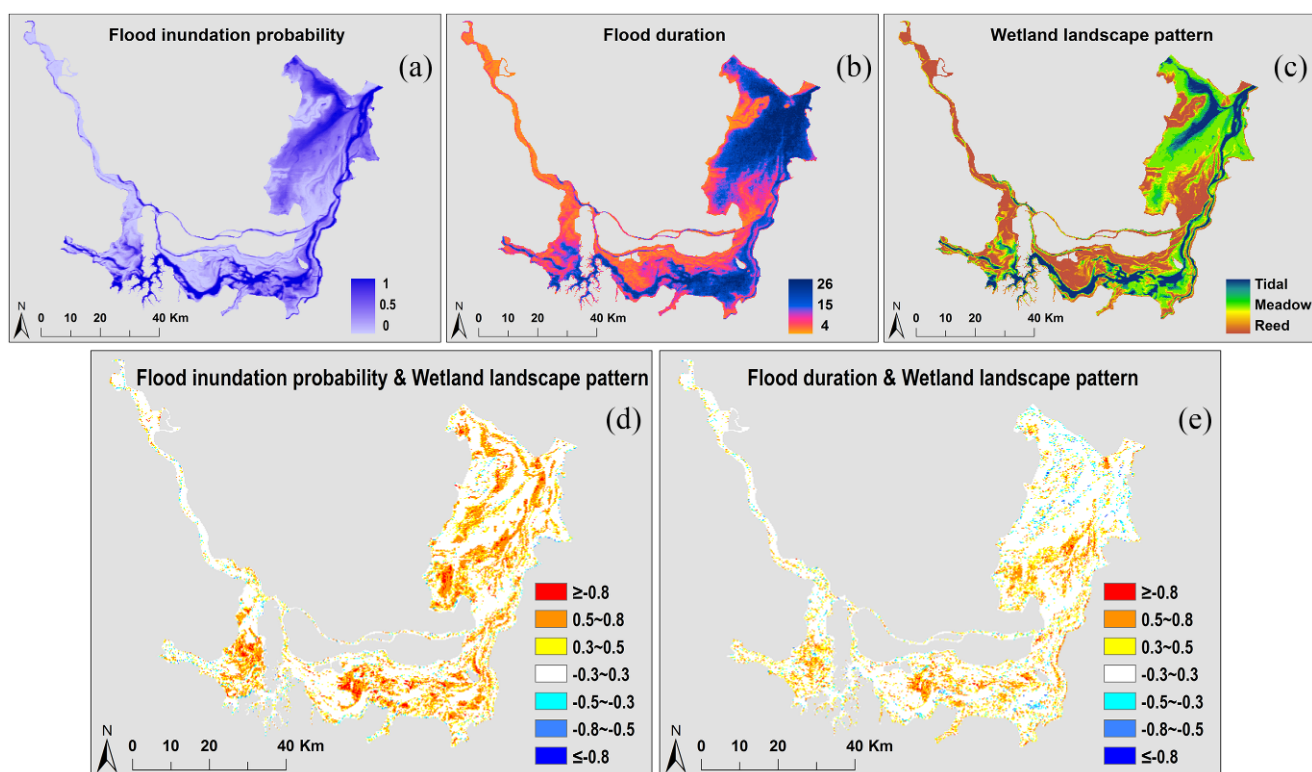


Figure 11. (a) Average flood inundation probability from 2000 to 2012; (b) Average flood duration between 2000 and 2012; (c) Average wetland landscape pattern over the period 2000 to 2012; (d) Spatial correlation between flood inundation probability and wetland landscape pattern over the period 2000 to 2012; (e) Spatial correlation between flood duration and wetland landscape pattern over the period 2000 to 2012.

First, approximately 65.9% of wetlands had weak correlations with flood inundation probability, and almost 76.0% of wetlands had weak correlations with flood duration. These areas with weak correlation coefficients were principally stable wetlands with small water-level gradients, in which wetland landscape pattern experienced insignificant changes over the 13-year period.

Second, nearly 32.2% of wetlands were positively correlated with flood inundation probability. Specifically, 12.9%, 16.8%, and 2.5% of wetlands had low, moderate, and highly significant correlations with it, respectively. Only 0.4% of wetlands were negatively associated with flood inundation probability. For flood duration, approximately 20.8% of wetlands were positively correlated with it. Specifically, 11.7%, 8.4%, and 0.7% of wetlands had low, moderate, and highly significant correlations with it, respectively. Only 0.6% of wetlands were negatively related to flood duration. Regions with strong correlation coefficients were primarily distributed in areas with large water level gradients, in which wetlands were greatly influenced by inter-annual fluctuations of water level. These areas were transitional zones between meadow and tidal wetlands or between meadow and reed wetlands. Water-level gradient determined the survival boundary of wetland vegetation. Regions with high correlation coefficients were probably the areas with most potential to experience vegetation succession.

Overall, flood inundation probability presented a generalized influence on wetland landscape patterns, whereas flood duration induced a local effect on wetland vegetation. Wetlands having high correlations with flood inundation probability included all types of wetland vegetation, whereas those holding significant correlations with flood duration were primarily a small fraction of reed and meadow wetlands. To some extent, flood inundation probability determined the general distribution of wetland vegetation, whereas flood duration specified the areas that are susceptible to flooding with large seasonal variations.

6. Discussion

6.1. Development of Flood Regimes and Their Influences on Wetland Landscape Patterns

Except for average annual cases, further analyses were conducted to examine the development of related parameters of flood regimes in three specified periods from 2000 to 2012, such as April, October, and June to September. Two chief considerations in determining the three such periods were the growing season of wetland plants in the Dongting Lake and the discharging or impounding time of the Three Gorges Reservoir. The results are shown in Figure 12.

In April, the inundation area experienced a decrease during 2000 to 2012, with a rate of $111.46 \text{ km}^2 \cdot \text{year}^{-1}$. However, the flood inundation probability experienced a slight increase between 2000 and 2012, with a rate of 0.0086 year^{-1} . The flood duration also increased sharply, with a rate of $0.10 \text{ day} \cdot \text{year}^{-1}$. The start/end date of the largest flood occurred early over the period from 2000 to 2012. These changes in wetland environment would increase areas of exposed wetlands with middle-high flood inundation probability and, thus, would promote the growth of meadows and improve the biodiversity of vegetation communities.

In October, the inundation area decreased during 2000 to 2012, with a rate of $23.18 \text{ km}^2 \cdot \text{year}^{-1}$. However, flood inundation probability and flood duration presented an opposite trend, which increased

slightly over the 13-year period. The start/end date of the greatest flood had a development of starting/ending ahead of time between 2000 and 2012. These changes were caused by the decreased water supplies in the Dongting Lake with the reduction in leakage flow from the Three Gorges Reservoir. Therefore, low wetlands would be exposed earlier than usual years, which could provide favorable conditions for the expansion of meadows. Given that the biomass accumulation of reed wetlands had been completed during this period, the changing water level would have insignificant effects on the yield of reeds.

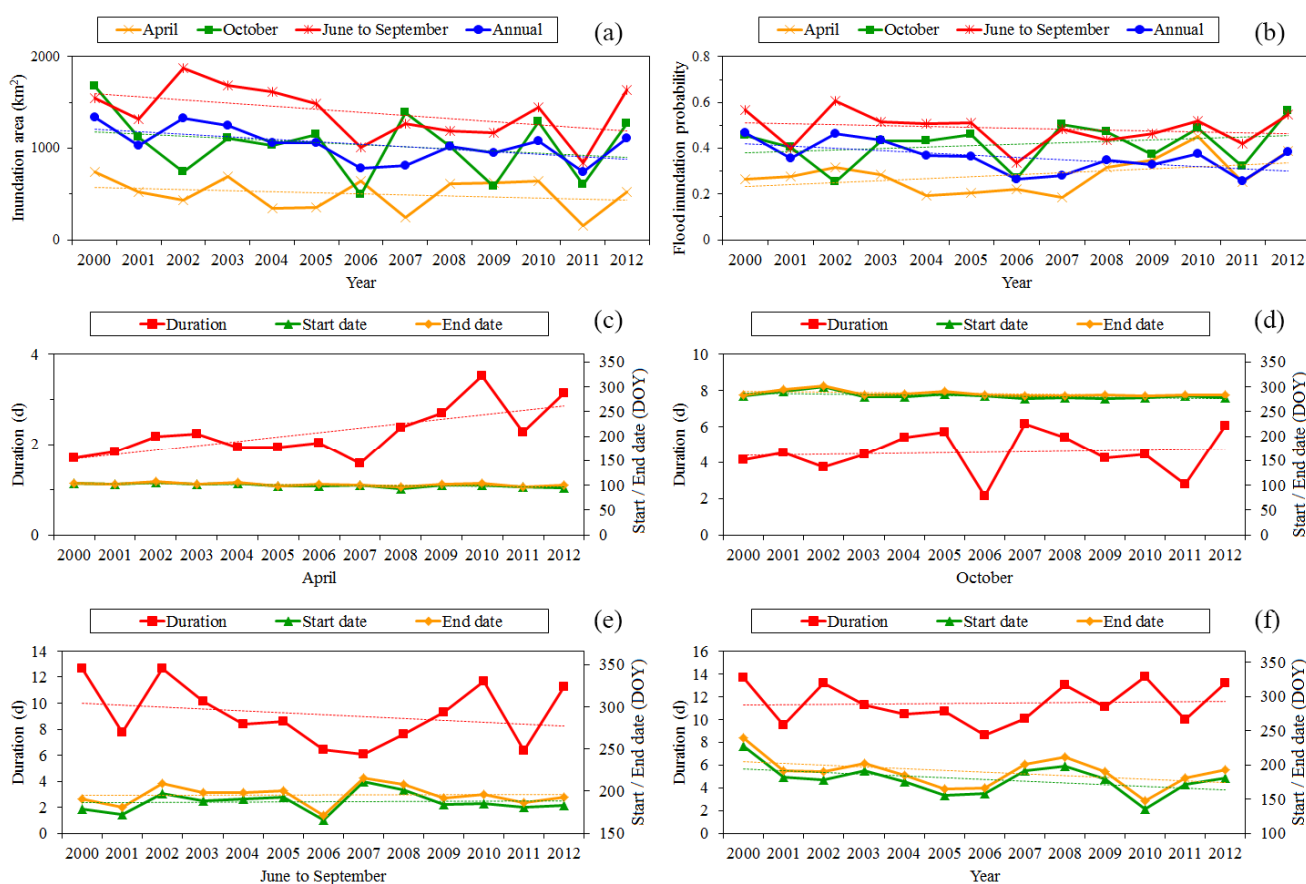


Figure 12. (a) Development of average inundation areas in April, October, June to September and each year from 2000 to 2012 in the Dongting Lake; (b) Development of average flood inundation probability in April, October, June to September and each year between 2000 and 2012; (c) Development of the average duration and start/end date of the largest flood in April during 2000 to 2012; (d) Development of the average duration and start/end date of the greatest flood in October from 2000 to 2012; (e) Development of the average duration and start/end date of the largest flood in June to September between 2000 and 2012; (f) Development of the average annual duration and start/end date of the greatest flood during 2000 to 2012. The dotted lines denote their development trends.

During June to September, inundation area, flood inundation probability, and flood duration all presented a consistent decrease from 2000 to 2012, with rates of $34.24 \text{ km}^2 \cdot \text{year}^{-1}$, 0.004 year^{-1} , and $0.15 \text{ day} \cdot \text{year}^{-1}$, respectively. The start/end date of the largest flood had a slight delay trend over the period during 2000 to 2012. These changes demonstrated the regulation of the Three Gorges Reservoir

by weakening flood peaks in flood seasons. Considering that the majority of wetland plants were completely submerged in flood periods, fluctuations in inundation area, flood inundation probability, and flood duration would have an inconsiderable influence on wetland vegetation communities.

Both annual inundation area and annual flood inundation probability experienced a downward trend between 2000 and 2012, with rates of $27.65 \text{ km}^2 \cdot \text{year}^{-1}$ and 0.01 year^{-1} , respectively. The start/end date of the greatest flood occurred early over the period from 2000 to 2012, shifting to an earlier date of $2.48/2.49 \text{ day} \cdot \text{year}^{-1}$. Flood duration fluctuated and remained stable over the period during 2000 to 2012.

Overall, inundation areas in the above four periods experienced a downward trend after the impoundment of the Three Gorges Reservoir in the Dongting Lake. Flood inundation probability declined between 2000 and 2012, presenting a decrease in the flood period (June to September), and experienced an upward trend in the normal period (April and October). Flood duration remained stable during 2000 to 2012, presenting a consistent decrease in the flood period and increase in the normal period. The start/end date of the largest flood in April, October, and each year all occurred early, except for the flood period. The succession of wetland vegetation generally resulted from the gradual accumulation of changes in the wetland environment for long periods of time. Given that the freshwater flowing into the Dongting Lake experienced a consistent decrease, those dominant wetland communities (meadows and reeds) were expected to invade the living space of submerged plants. The present wetland landscape pattern would be damaged and present forward succession in the Dongting Lake.

6.2. Changes in Wetland Landscape Patterns after the Flood Period

NDVI was introduced to characterize the growth and biomass of wetland vegetation before and after the flood period. This approach provides a clear way to understand the impact of flooding on wetland landscape patterns. NDVI is the most commonly used vegetation index with a range from -1 to 1 [70,71]. This index can be calculated as follows:

$$NDVI = (R_{nir} - R_r) / (R_{nir} + R_r) \quad (6)$$

where r and nir denote the first band and the second band of MODIS data, respectively. Studies have illustrated that NDVI had significant correlations with biomass, vegetation coverage, leaf area index (LAI) and other vegetation-related parameters [72].

Great changes can be found in wetland landscape patterns and NDVI values after the flood period (Figure 13). First, the phenomenon of wetland vegetation growing along the water-level gradient became evident after the flood period. A certain part of reed wetlands submerged in floods were replaced with meadow wetlands after the flood period. Therefore, the extent of reed wetlands presented a decrease after the flood period, whereas the area of meadow wetlands expanded sharply. These changes primarily occurred in the lower marshlands near water bodies. Second, wetland patches became crushing and complex after the flood period. To some extent, the interference of floods enhanced the biodiversity of wetland ecosystem. Third, lower regions near water bodies had higher NDVI values than other areas after the flood period. Wetlands submerged in floods would be exposed and begin to grow again after the flood period. This phenomenon would lead to the new growing

meadows presenting high NDVI values. In addition, reed wetlands gradually blooming white flowers would show reduced NDVI values after the flood period.

6.3. Role of Flooding in Wetland Evolution, and Its Possible Effects on Vegetation Succession

Floods played a critical role in accelerating the process of erosion or sedimentation of wetlands, which would have significant influences on wetland evolution and vegetation succession. On the one hand, fine sediments transported by flood waters could provide opportunities for the accumulation of soil nutrients and organic matters. On the other hand, the deposition of sediment in wetlands was expected to raise the elevation and thus to decrease the flood inundation probability. In these cases, forward succession would tend to occur in wetland vegetation. Lower wetlands originally occupied by submerged plants and meadows would be inclined to grow with reeds or woody plants.

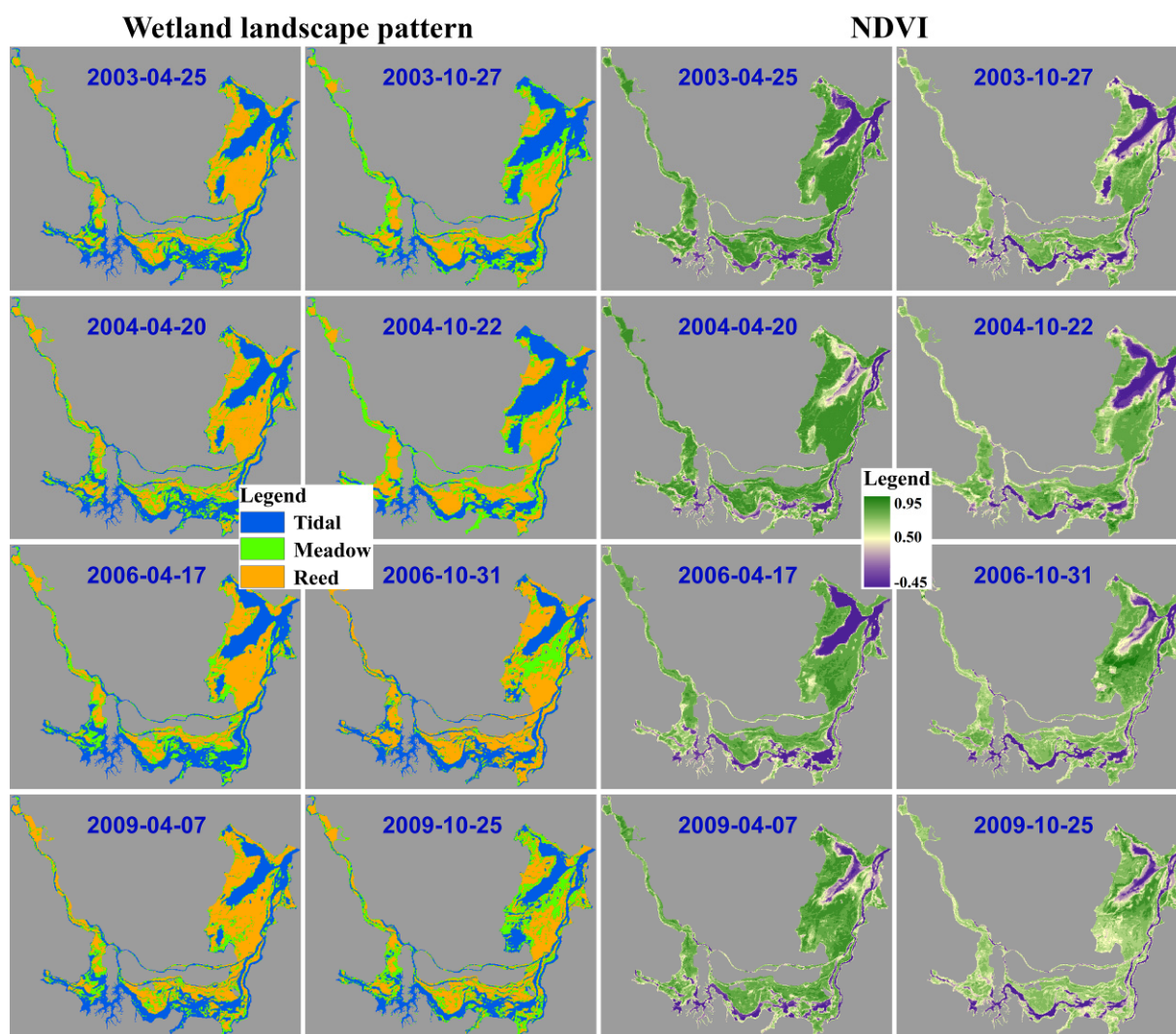


Figure 13. Changes in wetland landscape patterns and NDVI values of wetlands after the flood period.

Figure 14 gives an example of the process of wetland evolution and vegetation succession over the period from 1993 to 2010 in the region where the Ouchi River was flowing into the Dongting Lake.

Extents of reed and meadow wetlands expanded and were gradually moving forward to areas of tidal wetlands between 1993 and 2010. The injection point of the Ouchi River discharging into the Dongting Lake experienced a great evolution during 1993 to 2010, which was clearly indicated by the changes in locations of the yellow star in Figure 14. With the increase in wetland elevation, tidal wetlands had a tendency to be replaced with reed and meadow wetlands. Seasonal variations in spectral characteristics of remote sensing images were also presented. Meadow wetlands were difficult to distinguish from Landsat images in the normal season, whereas we can easily distinguish various types of wetlands from images in the dry period.

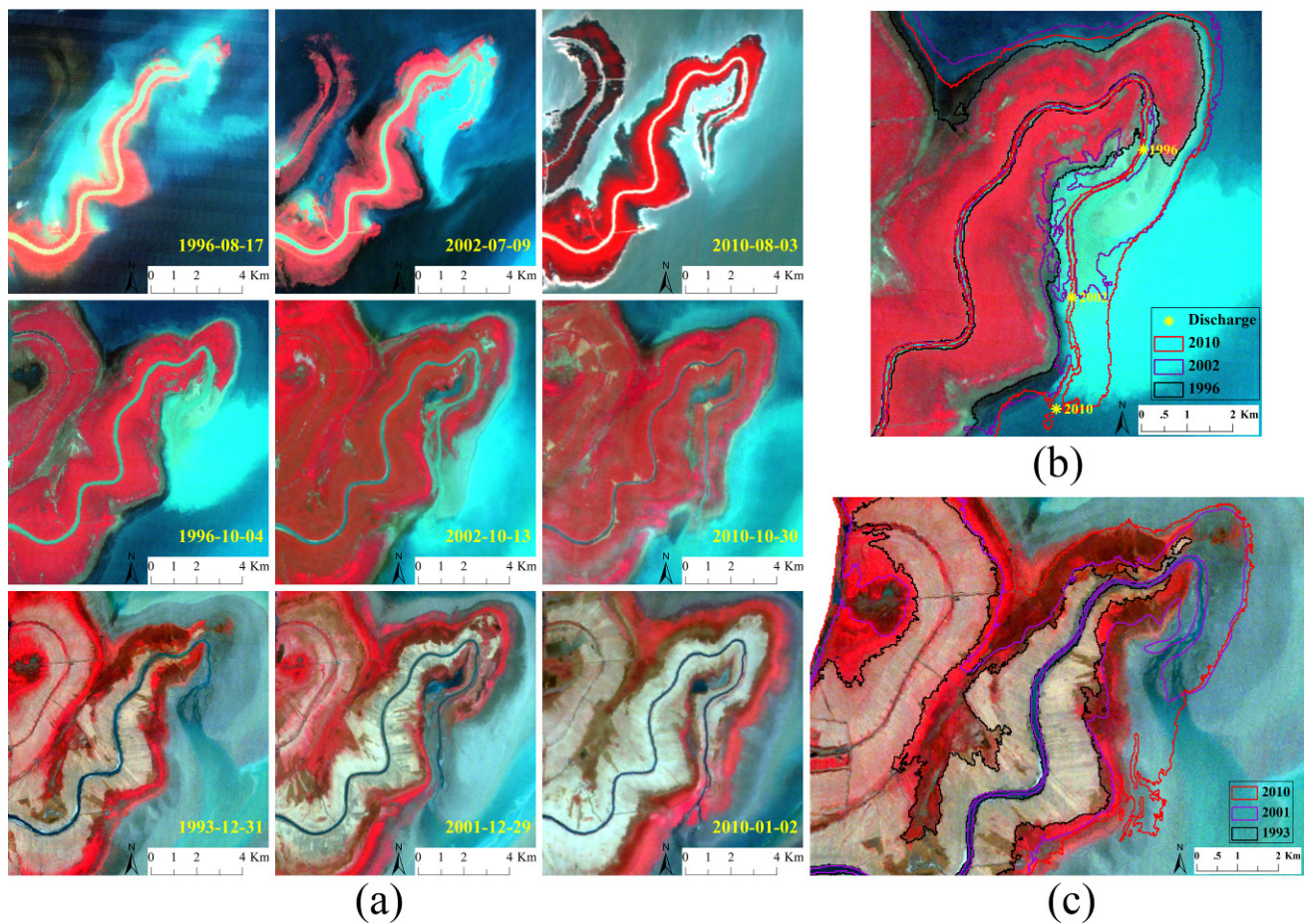


Figure 14. (a) Changes in spectral characteristics of remote sensing images in the region where the Ouchi River was flowing into the Dongting Lake in different seasons from 1993 to 2010. The underlying maps are Landsat false color composite images (4-3-2); (b) The evolution of boundaries between water and marshlands between 1996 and 2010 is presented. The base map is the Landsat image in 1996, and changes in locations of the yellow asterisk show the development of the injection point of the Ouchi River discharging into the Dongting Lake; (c) The evolution of reed wetlands during 1993 to 2010. The base map is the Landsat image in 1993.

Sediment diverted from the Yangtze River was the primary source of deposition in the Dongting Lake. The velocity of sediment deposition generally determined the wetland evolution and vegetation succession process. The sedimentation process was mitigated by the construction of the Three Gorges

Project, which would have positive effects on alleviating the shrink of the Dongting Lake. Some studies have demonstrated that sedimentary fluxes in the Dongting Lake experienced a downward trend after the impoundment of the Three Gorges Reservoir, and particle sizes and compositions of sediment tapered as well [2,73]. Given that sediments exported to the Yangtze River would still be less than those delivered to the lake, the Dongting Lake would be in a deposition situation with a reduced sedimentation rate for a long period. In other words, wetland vegetation in the Dongting Lake would be in a slow process of forward succession.

7. Conclusions

Several findings can be obtained from the analyses of MODIS time-series images over the 13-year period (from 2000 to 2012). Significant variations were identified in inundation extents at both inter-annual and seasonal scales in the Dongting Lake. Temporal changes in inundation areas derived from MODIS data were accordant with variations in annual and monthly runoff and precipitation data. Detailed explanations were obtained for spatial and temporal characteristics of flood inundation probability, duration and start/end date of the annual largest flood, and their relations to wetland landscape patterns. Correlation analyses were implemented to explore spatial-temporal relationships between these related parameters of flood regimes and wetland landscape patterns during 2000 to 2012. Results demonstrated that flood inundation probability determined the general distribution of wetland vegetation, whereas flood duration specified the areas that are susceptible to flooding with large seasonal variations. Further discussion included development of parameters associated with flood regimes and their influences on wetland landscape patterns after implementation of the Three Gorges Project, changes in wetland landscape patterns after the flood period, and the role of flooding in wetland evolution and its possible effect on vegetation succession. Two highlights of this study can be summarized below.

First, this study utilized MODIS time-series data to characterize spatial and temporal changes in flood regimes of the entire lake from a global viewpoint, which addressed the shortage in hydrological data with limited observation sites. Such utilization is an effective scheme for dynamically monitoring variations in wetland environment and for making convenient comparisons among different periods.

Second, quantitative analyses were conducted to evaluate varying degrees of the effect of flooding on changes in wetland landscape patterns on the basis of the 13-year MODIS images. Results of these analyses would be important scientific references for understanding the succession law of wetland vegetation and restoring wetland vegetation communities in the Dongting Lake.

Nevertheless, this study also has limitations. The accuracy of the estimated flood regime could be seriously affected by image quality and spatial resolution of MODIS data. Besides, validations of inundation extents and flood regimes using traditional ground truth information are impossible for lakes with drastic variations in water levels. We believe the problems will be resolved by the upcoming Surface Water Ocean Topography (SWOT) mission, which will provide simultaneous measurements of inundation extents and flood water elevations at both high spatial and temporal resolutions. Further research may focus on the effect of time intervals between two large floods on wetland landscape patterns. The methodology proposed in the present paper may be applied to highly dynamic lakes such as Poyang Lake, and will contribute to the water-resource management and the maintenance of

wetland ecosystems. Results from this research can provide baseline information to understand changes in wetland landscape patterns and their connections with flood events, human activities, as well as long-term climate change.

Acknowledgments

This research was supported by the “Strategic Priority Research Program–Climate Change: Carbon Budget and Related Issues” (Grant No.: XDA05050107) of the Chinese Academy of Sciences, Ministry of Environment Protection–Chinese Academy of Sciences Cooperation Program (Grant No.: STSN-01-06), and the “Ecology and Environment Information System for the Three Gorges Project” of the Institute of Remote Sensing Applications, Chinese Academy of Sciences. We also thank the anonymous reviewers for their detailed comments and suggestions.

Author Contributions

Yanxia Hu had the original idea for the study, processed the remote sensing images, and conducted the analysis. Jinliang Huang and Yun Du gave guidance for the organization and improvement of the manuscript. Pengpeng Han and Wei Huang provided valuable suggestions for the revision and were involved in the language polishing. The manuscript was written by Yanxia Hu with contributions from all authors.

Conflicts of Interest

The authors declare no conflict of interest.

References

1. Andel, J.V.; Bakker, J.P.; Grootjans, A.P. Mechanisms of vegetation succession: A review of concepts and perspectives. *Acta Bot. Neerl.* **1993**, *42*, 413–433.
2. Xie, Y.H.; Chen, X.S. Effects of Three-Gorge Project on succession of wetland vegetation in Dongting Lake. *Res. Agric. Mod.* **2008**, *29*, 684–687.
3. Zhao, B.; Yan, Y.E.; Guo, H.Q.; He, M.M.; Gu, Y.J.; Li, B. Monitoring rapid vegetation succession in estuarine wetland using time series MODIS-based indicators: An application in the Yangtze River Delta area. *Ecol. Indic.* **2009**, *9*, 346–356.
4. Fu, W.G.; Li, P.P.; Wu, Y.Y. Mechanism of the plant community succession process in the Zhenjiang Waterfront Wetland. *Plant Ecol.* **2011**, *212*, 1339–1347.
5. Ho, M.C.; Richardson, C.J. A five year study of floristic succession in a restored urban wetland. *Ecol. Eng.* **2013**, *61*, 511–518.
6. O'Donnell, J.; Fryirs, K.; Leishman, M.R. Can the regeneration of vegetation from riparian seed banks support biogeomorphic succession and the geomorphic recovery of degraded river channels? *River Res. Appl.* **2014**, doi:10.1002/rra.2778.
7. Palanisamy, B.; Chui, T.F.M. Understanding wetland plant dynamics in response to water table changes through ecohydrological modelling. *Ecohydrology* **2013**, *6*, 287–296.

8. Rosenzweig, C.; Tubiello, F.N.; Goldberg, R.; Mills, E.; Bloomfield, J. Increased crop damage in the US from excess precipitation under climate change. *Global Environ. Chang.* **2002**, *12*, 197–202.
9. Voesenek, L.A.C.J.; Rijnders, J.H.G.M.; Peeters, A.J.M. Plant hormones regulate fast shoot elongation under water from genes to communities. *Ecology* **2004**, *85*, 16–27.
10. Bai, J.H.; Ouyang, H.; Yang, Z.F.; Cui, B.S.; Cui, L.J.; Wang, Q.G. Changes in wetland landscape patterns: A review. *Progr. Geog.* **2005**, *24*, 36–45.
11. Broen, M.T. A simulation model of hydrology and nutrient dynamics in wetlands. *Comput. Environ. Urban Syst.* **1988**, *12*, 221–237.
12. Coates, R.; Swanson, M.; Williams, P. Hydrologic analysis for coastal wetland restoration. *Environ. Manag.* **1989**, *13*, 715–727.
13. Wu, C.D.; Meng, X.M.; Chu, J.Y.; Fu, W.G.; He, H.J.; Meng, X.J. Correlation between hydrological situation and vegetation in Mount Beigu wetland. *J. Jiangsu Univ.* **2005**, *26*, 331–335. (In Chinese)
14. Li, J.B.; Dai, Y.; Ou, C.M.; Peng, P.; Deng, C.X. Effects of store water application of the three gorges reservoir on Yangtze River on water and sediment characteristics in the Dongting Lake. *J. Soil Water Conserv.* **2011**, *25*, 215–219.
15. Yao, S.M.; Lu, J.Y. Research on water and sediment transport characteristics downstream the Three Gorges Reservoir before and after its impoundment. *J. Hydroelectr. Eng.* **2011**, *30*, 117–123.
16. Cai, Q.H. The Dongting Lake and Three Gorges Project. *Yangtze River* **2012**, *43*, 1–4. (In Chinese)
17. Lai, X.J.; Jiang, J.H.; Huang, Q. Water storage effects of Three Gorges Project on water regime of Poyang Lake. *J. Hydroelectr. Eng.* **2012**, *31*, 132–148.
18. Huang, Q.; Jiang, J.H.; Lai, X.J.; Sun, Z.D. Changes of landscape structure in Dongting Lake wetlands and the evaluation on impacts from operation of the three gorges project. *Yangtze Basin Resour. Environ.* **2013**, *22*, 922–927.
19. Toner, M.; Keddy, P. River hydrology and riparian wetlands: A predictive model for ecological assembly. *Ecol. Appl.* **1997**, *7*, 236–246.
20. Chambers, R.M.; Smith, S.V.; Hollibaugh, J.T. An ecosystem-level content for tidal exchange studies in salt marshes of Tomales Bay, California, USA. In *Global Wetlands: Old World and New*; Mitsch, W.J., Ed.; Elsevier: Amsterdam, The Netherlands, 1994; pp. 265–276.
21. Dame, R.F. The net flux of materials between marsh-estuarine systems and the sea: The Atlantic coast of the United States. In *Global Wetlands: Old World and New*; Mitsch, W.J., Ed.; Elsevier: Amsterdam, The Netherlands, 1994; pp. 295–302.
22. Dame, R.F.; Lefeuvre, J.C. Tidal exchange: Import-export of nutrients and organic matter in new and old world salt marshes: Conclusions. In *Global Wetlands: Old World and New*; Mitsch, W.J., Ed.; Elsevier: Amsterdam, The Netherlands, 1994; pp. 181–201.
23. Duan, Y.; Li, Q.S.; Yang, F.; Li, X.C.; Zhang, H.P.; Li, Y. Study on the effects on wetlands in flooded area caused by transportation of sediment in floodwater. *Sci. Technol. Eng.* **2004**, *4*, 967–971.
24. Lu, X.L.; Deng, W. Review of flood effect on wetland system. *Wetland Sci.* **2005**, *3*, 136–142.

25. Liang, J.; Cai, Q.; Guo, S.L.; Xie, G.X.; Li, X.D.; Huang, L.; Zeng, G.M.; Long, Y.; Wu, H.P. MODIS-based analysis of wetland area responses to hydrological processes in the Dongting Lake. *Acta Ecol. Sin.* **2012**, *32*, 6628–6635.
26. You, H.L. Research on Effect of Water Regime on the Growth and Spatial Pattern of Wetland Vegetation in Poyang Lake. Ph.D. Thesis, The University of Chinese Academy of Sciences, Beijing, China, 2014.
27. Mishra, D.; Narumalani, S.; Lawson, M.; Rundquist, D. Bathymetric mapping using IKONOS multispectral data. *Gisci. Remote Sens.* **2004**, *41*, 301–321.
28. Fricker, H.A.; Scambos, T.; Carter, S.; Davis, C.; Haran, T.; Joughin, I. Synthesizing multiple remote-sensing techniques for subglacial hydrologic mapping: Application to a lake system beneath MacAyeal Ice Stream, West Antarctica. *J. Glaciol.* **2010**, *56*, 187–199.
29. Chormanski, J.; Okruszko, T.; Ignar, S.; Batelaan, O.; Rebel, K.T.; Wassen, M.J. Flood mapping with remote sensing and hydrochemistry: A new method to distinguish the origin of flood water during floods. *Ecol. Eng.* **2011**, *37*, 1334–1349.
30. Schumann, G.J.P.; Neal, J.C.; Mason, D.C.; Bates, P.D. The accuracy of sequential aerial photography and SAR data for observing urban flood dynamics, a case study of the UK summer 2007 floods. *Remote Sens. Environ.* **2011**, *115*, 2536–2546.
31. Klemas, V. Remote sensing of wetlands: Case studies comparing practical techniques. *J. Coastal Res.* **2011**, *27*, 418–427.
32. Long, C.M.; Pavelsky, T.M. Remote sensing of suspended sediment concentration and hydrologic connectivity in a complex wetland environment. *Remote Sens. Environ.* **2013**, *129*, 197–209.
33. Kuenzer, C.; Guo, H.D.; Huth, J.; Leinenkugel, P.; Li, X.W.; Dech, S. Flood mapping and flood dynamics of the Mekong delta: Envisat-ASAR-WSM based time series analyses. *Remote Sens.* **2013**, *5*, 687–715.
34. Sakamoto, T.; van Nguyen, N.; Kotera, A.; Ohno, H.; Ishitsuka, N.; Yokozawa, M. Detecting temporal changes in the extent of annual flooding within the Cambodia and the Vietnamese Mekong Delta from MODIS time-series imagery. *Remote Sens. Environ.* **2007**, *109*, 295–313.
35. Feng, L.; Hu, C.M.; Chen, X.L.; Cai, X.B.; Tian, L.Q.; Gan, W.X. Assessment of inundation changes of Poyang Lake using MODIS observations between 2000 and 2010. *Remote Sens. Environ.* **2012**, *121*, 80–92.
36. Huang, C.; Chen, Y.; Wu, J. Mapping spatio-temporal flood inundation dynamics at large river basin scale using time-series flow data and MODIS imagery. *Int. J. Appl. Earth Obs.* **2014**, *26*, 350–362.
37. Ordoyne, C.; Friedl, M.A. Using MODIS data to characterize seasonal inundation patterns in the Florida Everglades. *Remote Sens. Environ.* **2008**, *112*, 4107–4119.
38. Kuai, X.T.; Chen, D.Q.; Chen, Z.D. Application of MODIS L1B data to water resources. *Geospatial Inf.* **2006**, *4*, 41–43.
39. Li, J.G.; Li, J.R.; Huang, S.F.; Zuo, C.G. Application of Terra/MODIS time series data in dynamic monitoring of lake water area variations. *J. Nat. Resour.* **2009**, *24*, 923–933.
40. Zhou, H.; Mao DH.; Liu, P.L. The investigation on water lever of East Dongting Lake affected by Three-Gorge Reservoir. *T. Oceanol. Limnol.* **2014**, *4*, 180–186.

41. Li, Z.W.; Zhao, X.N.; Xie, G.X.; Yuan, M.; Jiang, Y.S. Water environmental quality properties of Dongting Lake affected by construction of the Three Gorges Project. *Geogr. Res.* **2013**, *32*, 2021–2030.
42. Long, Y. The spatial distribution and adaptability analysis of vegetation and its biomass in East Dongting Lake Wetland and the influence of Three Gorges Project. Master's Thesis, Hunan University, Changsha, China, 2013.
43. Li, J.B.; Dai, Y.; Yin, R.X.; Yang, Y.; Li, Y.D.; Wang, K.Y. Effects of Three Gorges Reservoir impoundment on the wetland ecosystem service value of Dongting Lake' South-Central China. *Chin. J. Appl. Ecol.* **2013**, *24*, 809–817.
44. Wang, S.M.; Dou, H.S.; Chen, K.Z.; Wang, X.C.; Jiang, J.H. *The History of Chinese Lakes*, 1st ed.; Science Press: Beijing, China, 1998; pp. 179–183.
45. Shi, X.; Xiao, W.H.; Wang, Y.; Wang, X. Characteristics and factors of water level variations in Dongting Lake during the recent 50 years. *South-North Water Diversion Water Sci. Technol.* **2012**, *10*, 18–22. (In Chinese)
46. Grime, J.P. Evidence for the existence of three primary strategies in plants and its relevance to ecological and evolutionary theory. *Amer. Nat.* **1977**, *111*, 1169–1194.
47. Blom, C.W.P.M.; Voeselek, L.A.C.J. Flooding: The survival strategies of plants. *Trends Ecol. Evol.* **1996**, *11*, 290–295.
48. Trebino, H.J.; Chaneton, E.J.; Leon, R.J.C. Flooding, topography, and successional age as determinants of species diversity in old-field vegetation. *Can. J. Bot.* **1996**, *74*, 582–588.
49. Wang, H.Y.; Chen, J.K.; Zhou, J. Influence of water level gradient on plant growth reproduction and biomass allocation wetland plant species. *Acta Phytoecol. Sin.* **1999**, *23*, 269–274.
50. Casanova, M.T.; Brock, M.A. How do depth, duration and frequency of flooding influence the establishment of wetland plant communities. *Plant Ecol.* **2000**, *147*, 237–250.
51. Tan, X.J.; Zhao, X.S. Spatial distribution and ecological adaptability of wetland vegetation in Yellow River Delta along a water table depth gradient. *Chin. J. Ecol.* **2006**, *25*, 1460–1464.
52. Liu, X.Z.; Ye, J.X. *Jiangxi Wetlands*, 1st ed.; China Forestry Press: Beijing, China, 2000. (In Chinese)
53. Yuan, Z.K. *Resources and Environment of Wetland in Dongting Lake*, 1st ed.; Hunan Normal University Press: Changsha, China, 2008. (In Chinese)
54. NASA. EOSDIS, NASA's Earth Observing System Data and Information System. Available online: <https://reverb.echo.nasa.gov/> (accessed on 4 June 2015).
55. MODIS Reprojection Tool. Available online: https://lpdaac.usgs.gov/tools/modis_reprojection_tool/ (accessed on 4 June 2015).
56. Pohl, C.; van Genderen, J.L. Review article Multisensor image fusion in remote sensing: Concepts, methods and applications. *Int. J. Remote Sens.* **1998**, *19*, 823–854.
57. USGS. Landsat Missions. Available online: <http://landsat.usgs.gov/> (accessed on 4 June 2015).
58. China Meteorological Data Sharing Service System. Available online: <http://cdc.nmic.cn/> (accessed on 4 June 2015). (In Chinese)
59. Changjiang Water Resources Commission of the Ministry of Water Resources. The bulletin of the Sediments. Available online: <http://www.cjw.com.cn/zwzc/bmgb/nsgb/> (accessed on 4 June 2015). (In Chinese)

60. Hu, Y.X.; Huang, J.L.; Du, Y.; Han, P.P.; Wang, J.L.; Huang, W. Monitoring wetland vegetation pattern response to water-level change resulting from the Three Gorges Project in the two largest freshwater lakes of China. *Ecol. Eng.* **2014**, *74*, 274–285.
61. Ceccato, P.; Gobron, N.; Flasse, S.; Pinty, B.; Tarantola, S. Designing a spectral index to estimate vegetation water content from remote sensing data: Part 1. Theoretical approach. *Remote Sens. Environ.* **2002**, *82*, 188–197.
62. Sawaya, K.E.; Olmanson, L.G.; Heinert, N.J.; Brezonik, P.L.; Bauer, M.E. Extending satellite remote sensing to local scales: Land and water resource monitoring using high-resolution imagery. *Remote Sens. Environ.* **2003**, *88*, 144–156.
63. Feyisa, G.L.; Meilby, H.; Fensholt, R.; Proud, S.R. Automated Water Extraction Index: A new technique for surface water mapping using Landsat imagery. *Remote Sens. Environ.* **2014**, *140*, 23–35.
64. Deering, D.W. Rangeland Reflectance Characteristics Measured by Aircraft and Spacecraft Sensors. Ph.D. Thesis, Texas A&M University, College Station, TX, USA, 1978.
65. McFeeters, S.K. The use of the normalized difference water index (NDWI) in the delineation of open water features. *Int. J. Remote Sens.* **1996**, *17*, 1425–1432.
66. Xu, H.Q. Modification of normalized difference water index (NDWI) to enhance open water features in remotely sensed imagery. *Int. J. Remote Sens.* **2006**, *27*, 3025–3033.
67. Hu, C.M. A novel ocean color index to detect floating algae in the global oceans. *Remote Sens. Environ.* **2009**, *113*, 2118–2129.
68. Jian, X.; Chen, H.; Xing, Z.Y.; Feng, T.; Yin, L.Y. Influence of waterbody types on threshold of waterbody area extraction using remote sensing technology. *Sci. Technol. Eng.* **2014**, *18*, 267–274.
69. Roberts, L.G. Machine perception of three-dimensional solids, In *Optical and Electro-Optical Information Processing*; Tippet, J.T., Ed.; MIT Press: Cambridge, UK, 1965, pp. 157–161.
70. Silleos, N.G.; Alexandridis, T.K.; Gitas, I.Z.; Perakis, K. Vegetation indices: Advances made in biomass estimation and vegetation monitoring in the last 30 years. *Geocarto Int.* **2006**, *21*, 21–28.
71. Rouse, J.W.; Haas, R.W.; Schell, J.A.; Deering, D.W.; Harlan, J.C. Monitoring the Vernal Advancement and Retrogradation (Green Wave Effect) of Natural Vegetation. Available online: <http://ntrs.nasa.gov/archive/nasa/casi.ntrs.nasa.gov/19730017588.pdf> (accessed on 2 June 2015).
72. Zhao, Y.S. *Principles and Methods of the Application of Remote Sensing*, 1st ed.; Science Press: Beijing, China, 2003; pp. 373–374.
73. Ma, Y.X.; Lai, H.Z. Research on the variations of the water and sediment for recent 50 years in the Jingjiang River and Dongting Lake area. *Res. Soil Water Conserv.* **2005**, *12*, 103–106.